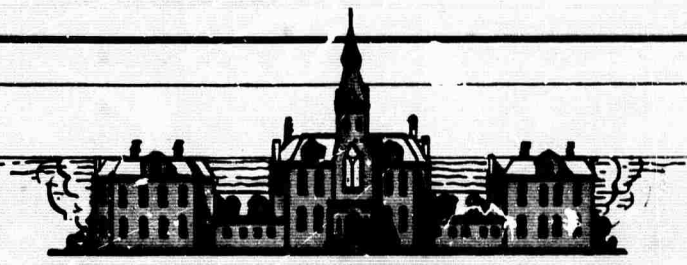
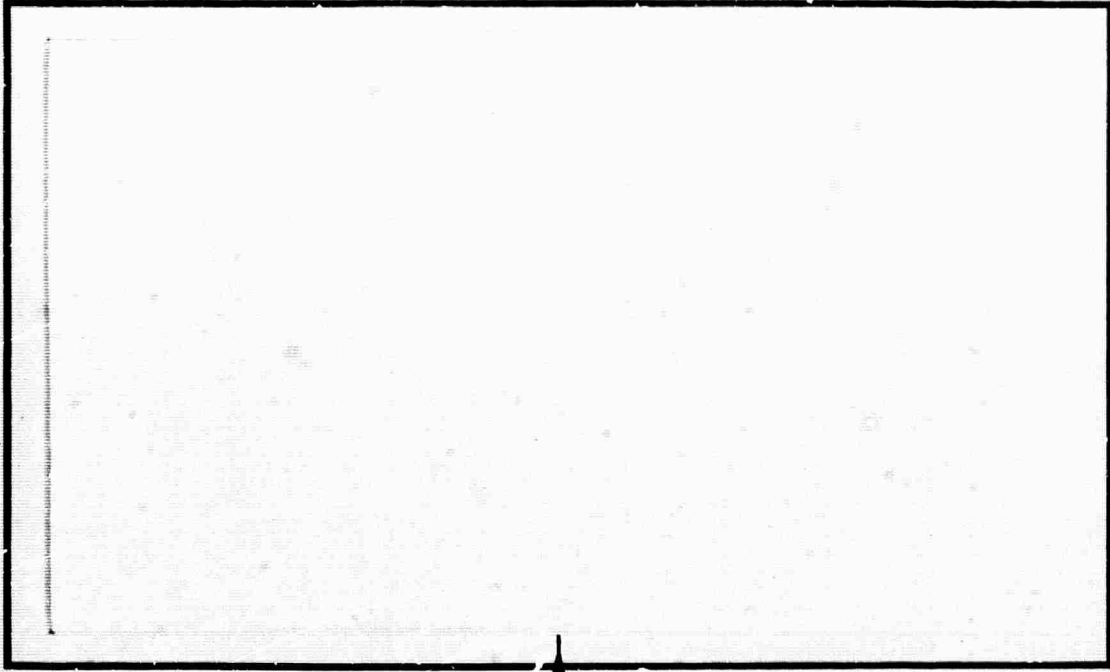
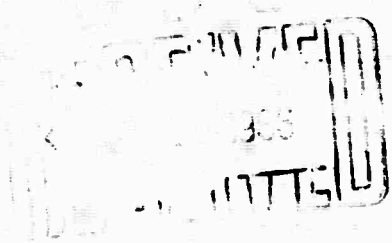


632014
A-632014



CLEARINGHOUSE FOR FEDERAL SCIENTIFIC AND TECHNICAL INFORMATION			
Hardcopy	Microfiche		
\$3.00	\$0.50	57 pp	as
ARCHIVE COPY			



Code 1

**KANSAS STATE UNIVERSITY
MANHATTAN, KANSAS**

ARPA Order Number ---- 306-62

Project Code Number -- 3730

SENSITIZED FLUORESCENCE*

FINAL REPORT

1 April 1963 to 31 December 1965

Prepared for

The Office of Naval Research

on Contract Nonr 3634(02)

**Submitted by: Basil Cumutte, Jr.
Professor of Physics
Kansas State University
Manhattan, Kansas**

***This research is a part of Project DEFENDER, under the joint sponsorship of the Advanced Research Projects Agency, the Office of Naval Research, and the Department of Defense**

CONTENTS

Table of Contents - - - - - 1
Abstract - - - - - ii
Introduction - - - - - 1
Laser Prospects - - - - - 4
Appendix I - - - - - I-1
Appendix II - - - - - II-1

Reproduction in whole or in part is permitted for any purpose of the
U. S. Government

Abstract

The quenching of mercury resonance fluorescence by thallium in a mercury-thallium vapor mixture has been measured to determine the quenching cross section of thallium for the 5^3P_1 state of mercury. The results of the quenching cross section (σ_d) measurements are tabulated below in Table I.

Table I

Quenching Cross Sections of Thallium for
the 6^3P_1 State of Mercury

<u>Temperature</u>	<u>σ_d</u>
800 ^o	34±13 A ²
850 ^o	31±8 A ²
900 ^o	25±6 A ²

The cross sections for the transfer of energy to several of the thallium excited states on collision of ground state thallium atoms with excited and metastable mercury atoms were determined by measurement of the relative intensities of thallium sensitized fluorescence radiation to mercury resonance fluorescence radiation. The excitation transfer cross sections determined from the measurements reported in Appendix II are tabulated in Table II for ease of reference.

Table II

Excitation Transfer Cross Sections from the Mercury 6^3P_1 and 6^3P_0 States to the Thallium $8^2S_{1/2}$ (σ_{7d}), $6^2D_{5/2,3/2}$ (σ_{56d}), and $7^2P_{3/2,1/2}$ (σ_{34d}) States

Temperature °C	Cross Section		
	σ_{7d} Å^2	σ_{56d} Å^2	σ_{34d} Å^2
800	0.7 ± 0.4	3.0 ± 1.0	5.6 ± 1.9
850	0.5 ± 0.2	3.6 ± 1.1	6.6 ± 2.1
900	0.4 ± 0.1	2.7 ± 0.8	7.4 ± 2.3

The implications of the magnitudes of these cross sections on the prospects for the use of a mercury-thallium vapor in a laser system are discussed.

Introduction

With the introduction of the collision pumped continuous gas laser interest in cross sections for collisions of the second kind has been renewed. The calculation of laser gain and output requires a knowledge of the appropriate cross sections, but the number of such cross sections reported in the literature is small. Cross sections are reported only for the transfer from metastable states of helium to excited states of neon and several other quenching gases⁽¹⁾ and for the transfer from mercury to several of the excited states of sodium⁽²⁾.

This study was undertaken to make use of the phenomenon of sensitized fluorescence to evaluate energy transfer cross sections from mercury to thallium.

The first part of the study was devoted to the evaluation of the de-excitation (quenching) cross section of thallium for the 6^3P_1 state of mercury. The quenching cross section, σ_d , was evaluated by measurements of the decrease in the resonance fluorescence of mercury in the presence of thallium. The details of the measurements and the analysis of the intensity data are given in Appendix I.

The second part of the study was the evaluation of the energy transfer cross sections for the transfer of energy from the mercury 6^3P_1 and 6^3P_0 states to various excited states of thallium. These cross sections were determined by the measurement of the ratio of the intensity of thallium sensitized fluorescence lines to the intensity of the mercury resonance fluorescence line. The details of the experimental arrangement, the measurements, and the analysis of the data are

given in Appendix II.

The excitation transfer cross sections reported in Appendix II are composite cross sections similar to the effective cross sections reported by Frisch and Kraulinya⁽³⁾. They are not constants dependent only on the atoms involved in the collision and the temperature. They are, however, expressed in terms of such basic cross sections in equations (23), (24), and (25) of Appendix II.

Using the notation of Appendix I and II we have the equations.

$$\sigma_{7d} = \sigma_{2007}^{ab} + \frac{n_1^a}{n_2^a} \sigma_{1007}^{ab} \quad (1)$$

$$\sigma_{56d} = (\sigma_{2006}^{ab} + \sigma_{2005}^{ab}) + \frac{n_1^a}{n_2^a} (\sigma_{1006}^{ab} + \sigma_{1005}^{ab}) \quad (2)$$

and

$$\sigma_{34d} = (\sigma_{2004}^{ab} + \sigma_{2003}^{ab}) + \frac{n_1^a}{n_2^a} (\sigma_{1004}^{ab} + \sigma_{1003}^{ab}) \quad (3)$$

From these equations we can see that even at a fixed temperature the composite cross sections, σ_{7d} , σ_{56d} , and σ_{34d} can vary depending on the ratio of the population of the metastable 6^3P_0 state to the population of the 6^3P_1 state of mercury. This ratio, $\frac{n_1^a}{n_2^a}$, can be changed by changing the number density of thallium since this decreases the rate of loss of metastable (6^3P_0) mercury atoms at the walls by decreasing the mean free path while leaving unchanged the rate of formation of excited (6^3P_1) mercury atoms.

As the temperature increases the number density of thallium increases causing the ratio $\frac{n_1^a}{n_2^a}$ to increase. If one looks at Table IV Appendix II he notes that the uncertainties make any inferences concerning temperature differences somewhat speculative. However, with some reservation one can draw the following tentative conclusion. The cross

section σ_{34d} increases with temperature contrary to the expected decrease because of the shorter collision times at the higher temperature. This would indicate that the term $\frac{n_f^a}{n_a^2} (\sigma_{1004}^{ab} + \sigma_{1003}^{ab})$ is dominant in determining this cross section and the increase with higher temperature is due to the increase in $\frac{n_f^a}{n_a^2}$. The cross section σ_{7d} decreases with temperature indicating that the term σ_{2007}^{ab} is dominant in determining the value for σ_{7d} .

The initial rise followed by a decrease in the cross section σ_{56d} with increasing temperature can be taken to indicate that all the terms in the right hand side of equation (2) are important in determining the value of σ_{56d} . The above tentative conclusions are in keeping with Winan's⁽⁴⁾ partial J selection rule. If the interaction is a central force interaction then the total angular momentum must remain constant during the interaction and energy transfer is restricted by this condition. Applying this rule we find that in collision with mercury in the 6^3P_1 state, a ground state thallium atom can only be raised to a $2^2S_{1/2}$, $2^2P_{1/2}$, $2^2P_{3/2}$ or a $2^2D_{3/2}$ state, while in collision with a mercury atom in the 6^3P_0 state the thallium atom can only be excited to the $2^2S_{1/2}$ and $2^2P_{1/2}$ states.

When one also adds to this partial J selection rule the requirement of near energy resonance between the initial state of mercury and the final state of thallium we can list the following as the mercury and thallium states between which energy transfer is most probable:

<u>Mercury State</u>	<u>Thallium State</u>	<u>ΔE (cm⁻¹)</u>
6 ³ P ₁	8 ² S _{1/2}	-454
6 ³ P ₁	6 ² D _{3/2}	-3292
6 ³ P ₁	7 ² P _{3/2}	-4249
6 ³ P ₁	7 ² P _{1/2}	-5250
6 ³ P ₀	8 ² S _{1/2}	+1104
6 ³ P ₀	7 ² P _{1/2}	-3492
6 ³ P ₀	7 ² S _{1/2}	-13164 .

From this table it appears that the largest basic energy transfer cross sections should be σ_{2007}^{ab} , σ_{2005}^{ab} , and σ_{1003}^{ab} . If these were the largest cross sections in equations (1-3) the observed temperature dependence of the cross sections would be expected. The partial J selection rule is not rigorously obeyed, however, since the interaction forces during collisions are not simple central forces and the rule can only be used as a guide to which cross sections may be expected to be large.

Laser Prospects

One can use the reported quenching and excitation transfer cross sections to find the relative rates for processes of interest in a mercury-thallium vapor mixture. Using the schematic diagram given in Figure 1, Appendix I, one can write the equilibrium rate equations for the pair of mercury states 6³P₁ and 6³P₀ considered as a composite state.

Without thallium present, in the notation of Appendix I,

$$O_{R02}^a = O_{R20}^a + O_{R10}^{aw} , \quad (4)$$

while with thallium present,

$$R_{02}^a = R_{20}^a + R_{10}^{aw} + R_7^{ab} + R_{56}^{ab} + R_{34}^{ab} \quad (5)$$

where

$$R_7^{ab} = R_{2007}^{ab} + R_{1007}^{ab} \quad (6)$$

$$R_{56}^{ab} = R_{2005}^{ab} + R_{1005}^{ab} + R_{2006}^{ab} + R_{1006}^{ab} \quad (7)$$

and,

$$R_{34}^{ab} = R_{2003}^{ab} + R_{1003}^{ab} + R_{2004}^{ab} + R_{1004}^{ab} \quad (8)$$

These equations can be manipulated to yield,

$$R_7^{ab}/R_{02}^a = \frac{\sigma_{7d}}{\sigma_d + (A_{20}^a/n_0^b v_{20}^{ab})} \quad (9)$$

$$R_{56}^{ab}/R_{02}^a = \frac{\sigma_{56d}}{\sigma_d + (A_{20}^a/n_0^b v_{20}^{ab})} \quad (10)$$

$$R_{34}^{ab}/R_{02}^a = \frac{\sigma_{34d}}{\sigma_d + (A_{20}^a/n_0^b v_{20}^{ab})} \quad (11)$$

$$R_{10}^{aw}/R_{02}^a = \frac{\sigma_d - \sigma_{7d} - \sigma_{56d} - \sigma_{34d}}{\sigma_d + (A_{20}^a/n_0^b v_{20}^{ab})} \quad (12)$$

and,

$$R_{20}^a/R_{02}^a = \frac{(A_{20}^a/n_0^b v_{20}^{ab})}{\sigma_d + (A_{20}^a/n_0^b v_{20}^{ab})} \quad (13)$$

From the values of σ_d , σ_{7d} , σ_{56d} , σ_{34d} , and $(A_{20}^a/n_0^b v_{20}^{ab})$ given in Appendix I and II and the use of equations (9-13) one can calculate the rates given in Table 1 as a percentage of the rate of excitation of the 6^3P_1 state of mercury by absorption of resonance radiation (R_{02}^a).

Table 1

Ratio of Rates of Several Processes as a Percentage of the Rate of Excitation of the Mercury 6^3P_1 State. The uncertainties in all values have been neglected in this table.

Temperature °C	R_{7}^{ab}	R_{56}^{ab}	R_{34}^{ab}	R_{10}^{aw}	R_{20}^a
800	0.2%	1.0%	1.9%	8.2%	88 %
850	0.3%	2.3%	4.3%	13.2%	79.9%
900	0.5%	3.7%	10.1%	19.9%	65.8%

The reported values of the energy output of a low pressure mercury vapor lamp⁽⁵⁾ allows one to calculate the number density of excited (6^3P_1) mercury atoms in the plasma of such a lamp. The calculated number density of 6^3P_1 mercury atoms in a lamp of this type is about 3×10^8 atoms/cm³. The rate of loss of excited mercury atoms by spontaneous radiation in such a lamp is about 3×10^{16} transitions/cm³ sec.

If a mercury-thallium vapor mixture was pumped optically by a mercury vapor lamp which completely surrounded the vapor mixture the equilibrium population of the 5^3P_1 mercury state in the vapor mixture would be very nearly the same as that in the surrounding lamp. Using the value 3×10^8 cm⁻³ for n_2^a one can calculate the rate of transfer of thallium atoms into the $7^2P_{3/2,1/2}$ states at 900°C as 4.6×10^{15} transitions/cm³ sec. From this collision pumping rate, one can calculate the equilibrium number densities in these two states and similarly calculate the population in other excited thallium states.

Assuming that spontaneous radiation processes provide the only rate of loss of excited thallium atoms one can arrive at the following number densities for the excited thallium states:

<u>States</u>	<u>Approximate Number Density</u>
$8^2S_{1/2}$	1×10^7
$6^2D_{5/3,3/2}$	$.6 \times 10^7$
$7^2P_{3/2,1/2}$	1.4×10^8

One can also use the calculated transition probabilities and the number densities given above to calculate the number density in the $7^2S_{1/2}$ state of thallium. This calculation yields a $7^2S_{1/2}$ population density of about 8×10^7 atoms/cm³. Thus, the excess population of the $7^2P_{3/2,1/2}$ states over that of the $7^2S_{1/2}$ state will be about 5×10^7 atoms/cm³. The expressions published by Ionescu-Pallas and Velculescu⁽⁶⁾ can also be used to estimate the population inversion of the $7^2P_{3/2,1/2}$ states over the $7^2S_{1/2}$ state and yields a result of about 2×10^7 cm⁻³.

The optical gain per unit length in a gas which has an inverted population is,

$$\alpha = \left(\frac{\ln 2}{16\pi^3} \right)^{1/2} \left(\frac{g_2 A_{2 \rightarrow 1} n}{c \nu^3 (\Delta \nu_d / \nu)} \right) \quad (14)$$

where,

$$n = \frac{n_2}{g_2} - \frac{n_1}{g_1} \quad ,$$

and n_1, n_2 = population densities in lower (1) and upper (2) laser levels.

g_1, g_2 = statistical weight of the levels

$A_{2 \rightarrow 1}$ = transition probability

ν = frequency of the transition

$\Delta \nu_d$ = Doppler line width, and

c = velocity of light.

Zare and Hershbach⁽⁷⁾ have shown that the gain expression simplifies to $\alpha \approx 10^{-12} n$, for a highly allowed transition at 400°K, which should be correct to within a factor of 2 for a mercury-thallium vapor mixture at 900°C. Using $n = 10^7$ we see that the gain per cm in a mercury-thallium vapor mixture at 900°C, with an excited mercury (6^3P_1) atom number density of $3 \times 10^8 \text{ cm}^{-3}$, should be about $\alpha \approx 10^{-5}$. In a one meter path length this would be a gain of .1% per pass which is just sufficient for oscillation. An increase in the excited mercury atom number density over that used in this estimate should be easily obtained, thus it should be possible to obtain a usable gain for a mercury-thallium vapor mixture on the $7^2P_{1/2} \rightarrow 7^2S_{1/2}$ or $7^2P_{3/2} \rightarrow 7^2S_{1/2}$ transitions.

If atoms were removed from the $7^2P_{3/2,1/2}$ states by stimulated emission at a rate equal to the rate of transfer in by collisions one can estimate the maximum power output per unit volume of the active vapor. This power output is calculated as $0.08 \text{ Joules/cm}^3/\text{sec}$ for a mercury-thallium vapor mixture in which the excited mercury atom number density is $3 \times 10^8 \text{ atoms/cm}^3$. For a laser 1 meter long with a 2 mm diameter resonant cavity one can calculate an upper limit of about 2.4 watts for the output in the $7^2P_{1/2,3/2} \rightarrow 7^2S_{1/2}$ transitions at 1.15μ and 1.30μ . This pair of transitions are the most favorable pair in the mercury-thallium vapor system without foreign gases present. If one could find another vapor which would strongly quench the $6^2P_{3/2}$ state of thallium preferentially, then the $7^2S_{1/2} \rightarrow 6^2P_{3/2}$ transition could be given consideration as a possible laser transition. The quenching of the $6^2P_{3/2}$ state involves an energy decrease of about 1.0 ev and at present one cannot suggest any vapor which would strongly quench this state and not quench other states more efficiently.

The prospects for the use of a mercury-thallium vapor mixture as the active medium for a laser of moderate power output on the $7^2P_{3/2} \rightarrow 7^2S_{1/2}$ and $7^2P_{1/2} \rightarrow 7^2S_{1/2}$ transitions are quite good. The sample cell preparation techniques reported in the second semi-annual technical report on this project can give one a guide as to the vacuum methods necessary to construct a suitable laser tube for a mercury-thallium vapor.

References

- 1- Benton, E. E., R. A. Matson, E. E. Ferguson, and W. W. Roberts, Phys. Rev. 128, 206, 1962.
- 2- Kraulinya, E. K., Opt. i Spektroskopiya, 17, 466, 1964.
- 3- Frish, S. E. and E. K. Kraulinya, Dokl. Akad. Nauk SSSR, 101, 837. 1955.
- 4- Winans, J., Rev. Mod. Phys., 16, 175, 1944.
- 5- Steeb, E. S. Jr. and W. E. Forsythe, in "Handbook of Physics", Editors, E. V. Condon and Hugh Odishaw, McGraw-Hill, New York, 1958.
- 6- Ionescu-Pallas, N. J. and V. G. Velcuiescu, Opt. i Spektroskopiya, 17, 139, 1964.
- 7- Zare, R. N. and D. R. Herschbach, Applied Optics, Supplement 2 1965. pp. 193-200.

APPENDIX I

Experimental Determination of the De-excitation Cross
Section for the 6^3P_1 State of Mercury by Thallium #
(submitted to the Physical Review for publication)

B. C. Hudson* and B. Curnutte, Jr.

Department of Physics, Kansas State University
Manhattan, Kansas

Abstract

The de-excitation or quenching cross section of thallium for the 6^3P_1 state of mercury has been obtained over a range of temperatures of 800°C to 900°C. Comparison of the resonance fluorescence from a mercury-thallium vapor mixture with the resonance fluorescence from a pure mercury vapor at the same number density, as determined by line absorption, allows the calculation of the de-excitation cross section. The present data together with Garrett's value of the lifetime of the 6^3P_1 state of mercury and existing data on the vapor pressures of mercury and thallium were used to obtain values of the de-excitation cross section. Values of the cross section range from $34 \pm 13A^2$ at 800°C to $25 \pm 6A^2$ at 900°C.

* This research supported in part by the Office of Naval Research and the Advanced Research Projects Agency and is a part of project DEFENDER.

* Present address: Lawrence Radiation Laboratories, Livermore, California.

Since the advent of the continuous gas laser there has been renewed interest in the processes whereby excitation energy can be transferred from one atom to another. Two manifestations of the transfer of excitation energy from one atomic species to another are: (a) a decrease in emission by the initially excited species, sometimes called quenching, and (b) an increase in emission from the species receiving the excitation energy, sometimes called sensitized fluorescence. Although there have been numerous studies of sensitized fluorescence of the mercury-thallium system¹, no measurements of the de-excitation cross section of thallium for the mercury 6^3P_1 state have been made. Few measurements of the absolute values of any excitation-transfer cross sections have been attempted², but Anderson and MacFarland³ have given relative transfer cross sections for the mercury-thallium system. The present study is concerned with the determination of the de-excitation cross section for transfer of energy out of the 6^3P_1 state of mercury as a result of collisions with unexcited thallium atoms.

Analysis

Figure 1 gives a schematic diagram of the pertinent portions of the energy level scheme for the mercury-thallium system. The mercury 6^1S_0 , 6^3P_0 and 6^3P_1 states are represented by the indices 0, 1, and 2, respectively, and the thallium $6^2P_{1/2}$, $6^2P_{3/2}$, $7^2S_{1/2}$, $7^2P_{1/2}$, $7^2P_{3/2}$, $6^2D_{3/2}$, $6^2D_{5/2}$ and $8^2S_{1/2}$ states are represented by the indices 0, 1, 2, 3, 4, 5, 6 and 7, respectively. When irradiated with 2537Å mercury resonance radiation, mercury atoms in a mixture of mercury and thallium vapor may absorb radiation and be raised to the 6^3P_1 state. These excited atoms may leave the excited state by spontaneous emission of 2537Å radiation or by a

radiationless transition resulting from collisions.

In treating the phenomena involved, it is desirable to adopt the following simple notation for the rates (number per unit volume per unit time) for various processes:

- (1) R_{ij}^a is the rate of an emission or absorption process by which Hg atoms are transferred from state i to state j .
- (2) R_{kl}^b is the rate of an emission or absorption process by which Tl atoms are transferred from state k to state l .
- (3) $R_{ij\ kl}^{ab}$ is the rate of a process involving collisions between Hg and Tl atoms in which the initial and final states of the Hg atom are i and j and the initial and final states of the Tl atom are k and l .
- (4) R_{ijpq}^{aa} is the rate of a process involving collisions between Hg atoms in which the initial and final states for one Hg atom are i and j while the initial and final states for the other Hg atom are p and q .
- (5) R_{ij}^{aw} is the rate for a process involving collisions of Hg atoms with the walls in which the initial and final states of the Hg atom are i and j .

With the above notation for the rates of the processes involved, the steady state equation for the rate of change of the population of the 6^3P_1 state can be written as

$$R_{02}^a = R_{20}^a + R_{2100}^{aa} + R_{2100}^{ab} + \sum_l R_{200l}^{ab} + R_{20}^{aw} \quad (1)$$

Under the experimental conditions encountered in the present work, the absorption rate R_{02}^a depends only on the intensity of the incident 2537Å radiation and the number density n_0^0 of ground-state mercury atoms. The rate

of spontaneous radiative transitions of mercury atoms from state 2 to state 0 is given by,

$$R_{20}^a = n_2^a \Lambda_{20}^a = n_2^a / \tau_{20}^a, \quad (2)$$

where Λ_{20}^a is the probability of spontaneous emission and τ_{20}^a is the radiative lifetime for state 2.

The rate of self-quenching of excited mercury atoms to the metastable state R_{2100}^{aa} is given by

$$R_{2100}^{aa} = n_2^a n_0^a \sigma_{2100}^{aa} v_{20}^{aa}, \quad (3)$$

where σ_{2100}^{aa} is the cross section^{4,5} for this process in which a mercury atom in the excited state 2 is transferred to the metastable state 1 as a result of a collision with a ground state mercury atom which does not change its state, the excess internal energy being converted into translational kinetic energy of the pair of atoms; and where the relative-velocity term

$$v_{20}^{aa} = [8\pi T (1/M_a + 1/M_a)]^{1/2}. \quad (4)$$

The rate R_{2100}^{ab} for transitions of Hg atoms from the excited state 2 to the metastable state 1 as a result of collisions between Hg atoms and Tl atoms in the ground state is given by

$$R_{2100}^{ab} = n_2^a n_0^b \sigma_{2100}^{ab} v_{20}^{ab}, \quad (5)$$

where σ_{2100}^{ab} is the cross section for the process and

$$v_{20}^{ab} = [8\pi T (1/M_a + 1/M_b)]^{1/2}. \quad (6)$$

The rate at which excited mercury atoms in collision with ground state thallium atoms produce excited thallium atoms in the ℓ -th state and leave the mercury atoms in the ground state is given by,

$$R_{200\ell}^{ab} = n_2^a n_0^b \sigma_{200\ell}^{ab} v_{20}^{ab}. \quad (7)$$

If the number density of mercury atoms in the ground state n_0^a , the temperature T , and the intensity of the incident 2537Å radiation are constant, then the absorption rate R_{02}^a with thallium present is equal to

${}^0R_{02}^a$, the absorption rate without thallium present, provided the partial pressure of thallium vapor is so low that pressure broadening of spectral lines is negligible and provided the intensity of the incident radiation is so low that n_1^a and n_2^a are negligible compared with n_0^a . Under these conditions, which are easily met, we may write,

$$R_{02}^a = {}^0R_{02}^a \quad (8)$$

Combining equations (8) and (1), we may write

$${}^0R_{20}^a + {}^0R_{2100}^{aa} + {}^0R_{20}^{aw} = R_{20}^a + R_{2100}^{aa} + R_{2100}^{ab} + \sum_l R_{200l}^{ab} + R_{20}^{aw} \quad (9)$$

With a gas sample in a volume sufficiently far removed from the walls, radiative decay or collision with another atom is far more likely for an excited atom than collision with the walls. Under such conditions the rates ${}^0R_{20}^{aw}$ and R_{20}^{aw} are negligible as compared with the other rates in (9) and can be eliminated from consideration.

From equations (2), (3), (5), and (7) we may write equation (9) as,

$$\begin{aligned} ({}^0n_2^a - n_2^a) / n_2^a = \tau_{20}^a [n_0^a \sigma_{2100}^{aa} v_{20}^{aa} - ({}^0n_2^a / n_2^a) n_0^a \sigma_{2100}^{aa} v_{20}^{aa} \\ + n_0^b \sigma_{2100}^{ab} v_{20}^{ab} + \sum_l n_0^b \sigma_{200l}^{ab} v_{20}^{ab}] \end{aligned} \quad (10)$$

According to Winans⁶, it is highly probable that σ_{2100}^{aa} is much smaller than σ_{200l}^{ab} . However, even if $\sigma_{2100}^{aa} = \sigma_{200l}^{ab}$, the first two terms on the right hand side of (10) are negligible with respect to the remaining terms, since for the conditions of the experiments reported here $r_0^b \gg n_0^a$, while n_2^a is of the same order of magnitude as ${}^0n_2^a$, and $v_{20}^{aa} \approx v_{20}^{ab}$. Making use of these conditions, we may write equation (10) in the following final form:

$$[\sigma_{2100}^{ab} + \sum_l \sigma_{200l}^{ab}] = (\tau_{20}^a v_{20}^{ab} n_0^b)^{-1} ({}^0n_2^a - n_2^a) / n_2^a = \sigma_d \quad (11)$$

where the term σ_d is called the de-excitation cross section and is the quantity of interest in the present study.

Although equation (11) is relatively simple, it is not in the most convenient form for calculation, since the quantities ${}^0n_2^a$ and n_2^a are not directly observable. However, the intensity I_{20}^a of resonance-fluorescence

radiation is related to the number density of atoms in the excited state n_2^a through the relationship,

$$I_{20}^a = K n_2^a, \quad (12)$$

where K is a quantity depending on the response of the monochromator and detecting system, the geometry, and the transition probability for emission of resonance radiation. Using equation (12) to express equation (11) in terms of measurable quantities, we find,

$$\sigma_d = (\tau_{20}^a n_0^b)^{-1} [8\pi RT(1/M_a + 1/M_b)]^{-1/2} (I_{20}^a / I_{20}^0 - 1), \quad (13)$$

provided K is kept constant.

The quantities in equation (13) are known or can be readily determined. The number density of ground state thallium atoms n_0^b can be obtained from the temperature of the coolest part of the container and the corresponding vapor pressure of thallium. The lifetime of the 6^3P_1 state τ_{20}^a has the value of 1.08×10^{-7} sec as determined by Garrett⁷. The ratio of the intensity of resonance fluorescence radiation from a pure mercury vapor to that of mercury vapor at the same density with added thallium was determined experimentally in the present study.

Experimental Arrangement

A schematic diagram of the experimental arrangement is shown in Figure 2. A cubical cell of fused quartz C is located at the center of a furnace MF. The source of 2537Å radiation is a temperature controlled "Pen-ray"⁸ low-pressure mercury lamp L. The 2537Å radiation from the lamp is collimated by a quartz lens and is incident on the cell through a window cut in a ceramic mask MA. The fluorescence radiation leaves the cell at right angles to the incident radiation through a window in the ceramic mask and is incident on the entrance slit of a Bausch and Lomb 500-mm grating monochromator M_1 , equipped with a 1P28 photomultiplier P_1 .

The transmitted 2537Å radiation leaves the cell through another window in the ceramic mask and is incident on the entrance slit of another Bausch and Lomb 500-mm grating monochromator M_2 , also equipped with a 1P28 photomultiplier PM_2 . The output of the lamp L is monitored by a third photomultiplier PM_3 after passing through a Baird-Atomic 2537Å Type A11 interference filter F which has a 250Å bandwidth at half peak transmission.

The sample cell is a 25-mm cube with a side arm reservoir 75 mm in length and was sealed after vacuum distillation of the desired amounts of mercury and thallium into the cell. Prior to the final distillation and sealing, the cell was outgassed at pressures of less than 5×10^{-8} torr and at temperatures above 1000°C . Each cell employed contained a small, fixed amount of mercury and a copious supply of thallium. At cell temperatures above 500°C the number density of mercury atoms was nearly constant and the number density of thallium atoms was determined by the temperature of the side arm, which was controlled by an auxiliary furnace SAF, in Fig. 2. In normal operation the side arm was maintained at a temperature 50°C below that of the main cell. With this temperature difference between the cell and the side arm, thallium condensation on the cell windows was eliminated.

The ceramic mask determined the geometry of irradiation within the cell and the volume from which the fluorescence radiation was detected. The dimensions of the windows in the mask are 10 mm by 1 mm and permit the vapor in the cell to be irradiated about 0.5 mm from one wall of the cell, as indicated in Fig. 2. The fluorescence radiation leaves the cell from a region about 1 mm from the point at which the incident 2537Å radiation enters the cell. At temperatures above 700°C , the 5350Å radiation from thallium was clearly visible from a well defined region along the path of

the incident 2537Å radiation. The dimensions and locations of the window in the ceramic mask were chosen in such a manner as to insure (1) that the 2537Å fluorescence radiation was primary resonance radiation and (2) that collisions of excited mercury atoms with the walls could safely be neglected.

The spectral slit widths of the monochromators were sufficiently large to pass all the radiation in the Doppler-broadened spectral lines being measured. The outputs of the photomultipliers PM_1 and PM_2 were amplified with an Engis SC1-10 dual-channel photomultiplier readout amplifier.

The number density of thallium atoms in the cell was determined from the known vapor pressure of thallium⁹ at the temperature of the side arm with appropriate ideal-gas-law correction for the 50°C higher temperature of the cell. The number density of mercury atoms was determined by comparison of the line-absorption in the sample cell with line absorption in a secondary cell containing pure mercury vapor at known pressures. The secondary cell was identical with cell C in Fig. 1; however, its side arm contained an excess of pure mercury. The side arm of the secondary cell was surrounded by a quartz jacket through which liquid nitrogen or water at temperatures in the range 0°C to 30°C could be circulated. With the side arm at liquid nitrogen temperature, the vapor pressure of Hg was negligibly low; with water in the jacket surrounding the side arm, the mercury vapor pressure was controlled by adjusting the temperature of the circulating water. The temperature of the secondary cell itself was maintained at 850°C. All temperatures were determined by the use of Leeds & Northrup Chromel-Alumel thermocouples, and the manufacture's calibration curves were employed. For temperatures below

100°C the thermocouple E.M.F. was recorded to ± 0.01 mV, which gives an uncertainty in the temperature of $\pm 0.25^\circ\text{C}$. For temperatures above 100°C the thermocouple E.M.F. was recorded to $\pm 0.25^\circ\text{C}$ mV, which gives an uncertainty of $\pm 6.25^\circ\text{C}$ for the high temperature readings. The number densities of mercury atoms in the side arm were computed from the known mercury vapor pressure⁹ at the temperature of the side arm; the number density of mercury in the secondary cell was computed from the side arm temperature and the temperature of the secondary cell by the use of the Knudsen effusion relationship.

The results of the measurements of absorption and resonance fluorescence of pure mercury vapor in the secondary cell are shown in Figure 3. Abscissa for both curves is the number density of mercury atoms in units of 10^{12} atoms/cm³, while the ordinate of Curve A represents percent absorption and the ordinate for Curve B gives the ratio of resonance fluorescent to the intensity of the beam transmitted by the evacuated cell. The symbol 0I_t represents the intensity of the transmitted beam of 2537Å radiation with mercury present but with no thallium present. The symbol I_0 represents the transmitted beam intensity with neither vapor present; i.e. with the mercury in the side arm frozen out by liquid nitrogen. Curve A marked $(1 - ^0I_t/I_0) \times 100$ represents the percentage of radiation which is absorbed by the mercury vapor in the cell, while the curve marked $(^0I_{20}^a/I_0)$ represents the ratio of the resonance fluorescence to the intensity of the beam transmitted by the evacuated cell. The near linearity of $(^0I_{20}^a/I_0)$ as a function of number density of mercury atoms indicates that radiation imprisonment is unimportant.

Results

Typical results of measurements on a cell containing a mercury-

thallium vapor are shown in Figure 4. The ordinate for curve A represents percent absorption and for curves B and C is the ratio of resonance-fluorescence intensity to the intensity of the beam transmitted by the evacuated cell, while the abscissa is the number density of thallium atoms in units of 10^{12} atoms/cm³ plotted on a logarithmic scale. Curve A, marked $(1 - I_t/I_0) \times 100$, and curve B, marked (I_{20}^a/I_0) , are the measured results from a cell containing a mercury-thallium vapor, while curve C, marked $({}^0I_{20}^a/I_0)$, gives the relative intensity of resonance fluorescence from a cell containing pure mercury vapor at the same mercury number density. Curve C in Fig. 4 is determined by using the value of $(1 - I_t/I_0) \times 100$ given in Curve A and finding from Fig. 3 the value of $({}^0I_{20}^a/I_0)$ to be expected in the absence of thallium.

Data similar to those shown in Fig. 4 were obtained with five cells, each of which contained a different amount of mercury. The results of the measurements are given in Table I. The first column of Table I gives the cell identifications. The second column gives the cell temperatures, which were measured to $\pm 6^\circ\text{C}$. The third column lists the number density of mercury atoms in the cell as determined by absorption measurements of the type presented in Fig. 3. The vapor pressure data⁹ were considered to contribute no error, but the uncertainty in the temperature measurements on which Fig. 3 is based introduced a $\pm 3\%$ uncertainty in the mercury number density. The fourth column of the table gives the number density of thallium atoms in the cell as determined from the side arm temperature. Because of the greater uncertainty in the measurement of high cell temperatures mentioned above, the uncertainty in the thallium number density is $\pm 12\%$. The fifth and sixth columns tabulate, respectively, the values of (I_{20}^a/I_0) and $({}^0I_{20}^a/I_0)$. The intensity ratio (I_{20}^a/I_0) was determined from chart recordings of the output of the photomultiplier readout amplifiers, while

the ratio $(^0I_{20}^a/I_0)$ was determined as described above. The ratios reported for I_{20}^a/I_0 and $^0I_{20}^a/I_0$ in Table I are averages for three sets of readings and have an uncertainty of ± 0.3 .

The seventh column lists the values of $(^0I_{20}^a - I_{20}^a)/I_{20}^a$ as computed from the intensity ratios of columns five and six. The eighth column tabulates the expected uncertainty in the values of $(^0I_{20}^a - I_{20}^a)/I_{20}^a$. This expected error was computed by taking the square root of the sum of the squares of the errors of the separate ratios as the error in the difference of the ratios $[(^0I_{20}^a/I_0) - (I_{20}^a/I_0)]$. The expected error in $[(^0I_{20}^a/I_0) - (I_{20}^a/I_0)]$ was converted to a percent error and the percent error in (I_{20}^a/I_0) was added to it giving the expected error in $[(^0I_{20}^a/I_0) - (I_{20}^a/I_0)]/(I_{20}^a/I_0) = (^0I_{20}^a - I_{20}^a)/I_{20}^a$, which is listed in column 8 of the table.

The ninth column gives the values for the de-excitation cross section σ_d . The uncertainties listed for σ_d include the uncertainty in $(^0I_{20}^a - I_{20}^a)/I_{20}^a$, the uncertainty in the number density of thallium atoms and a 5% uncertainty in the value of τ_{20}^a . The final values of σ_d as determined by these measurements and their uncertainties are: $34 \pm 13A^2$ at $800^\circ C$, $31 \pm 8A^2$ at $850^\circ C$ and $25 \pm 6A^2$ at $900^\circ C$. In view of the large uncertainties in these values, it is impossible to make valid inferences concerning possible temperature dependence of the cross section.

If we treat the variation of results from one cell to another at the same temperature as a statistical variation, the mean deviations are 25% in the $800^\circ C$ range, 15% in the $850^\circ C$ range and 18% in the $900^\circ C$ range. Since the mean deviations of σ_d as determined in each temperature range are about two-thirds of the average uncertainty, based on the least count of the measuring instruments, the internal consistency of the data appears

satisfactory.

The approximations made in the development of equation (13) require that (a) the loss of excited mercury atoms in wall collisions can be neglected, (b) the resonance fluorescence be primary resonance fluorescence, (c) the number density of ground-state thallium atoms greatly exceed the number density of ground state mercury atoms and (d) the geometry of the irradiation and detection system be kept constant.

Calculations based on the gas-kinetic cross sections indicate that at the lowest thallium vapor pressures for which cross sections were determined the mean free path in the cell was about 1 mm; this mean free path would thus permit mercury atoms to reach the walls, since the distance between the primary beam and the wall was 0.5 mm. However, at the atomic velocities involved an excited mercury atom travels only about 0.004 mm in one radiative lifetime; hence relatively few excited mercury atoms were lost in wall collisions.

For the measurements summarized in Table I the number density of mercury atoms was about 10×10^{12} atoms/cm³, corresponding to a pressure of about 2×10^{-4} mm Hg. At this pressure radiation imprisonment should be negligible, in view of the fact that the irradiated region was 0.5 mm from the window through which the fluorescence was measured. This conclusion is supported by the observation that with thallium in the cell the 5350Å sensitized fluorescence was clearly visible along the entire path of the incident 2537Å radiation.

The ratio n_0^b/n_0^a was greater than 100 for all situations for which cross sections were calculated.

The geometry was established by the construction of the sample cells, the use of a ceramic mask, and positioning of the source, cell, and

monochromators. No changes were made in the course of the experiments summarized in Table I.

The conditions used in the present experimental work, therefore, meet all the requirements necessary for the proper applicability of equation (13).

The de-excitation cross sections reported here are large and are of the order of magnitude of the reported quenching cross sections¹⁰ of large organic molecules for the 6^3P_1 state of mercury. If any appreciable fraction of this cross section is due to processes in which the thallium atoms are excited then it is likely that such collisions may be used to invert the thallium population distribution.

It might be remarked that the present method can be applied to other systems exhibiting sensitized fluorescence, provided the conditions necessary for the applicability of equation (13) are met, the lifetime of the excited state is known, and the number densities of the colliding atoms can be determined.

Acknowledgments

We would like to acknowledge the expert technical assistance of Mr. M. Ohno with the fabrication of the quartz cells and Mr. L. G. Phillips with the construction of equipment. We are indebted to Dr. Dudley Williams for his constructive criticism of the manuscript.

References

- 1- Franck, J., and G. Cario, Zeit. f. Phys., 17, 202-212, 1923.
 - Mrozowski, S., Acta Phys. Pol., 6, 58-67, 1937.
 - Swanson, R., and R. MacFarland, Phys. Rev., 98, 1063-1067, 1955.
 - Kraulinya, E. K., A. E. Lezdin, and Yu. A. Silin, Opt. i Spektroskopiya, 16, 154-156, 1965.
 - For a review of sensitized fluorescence up to 1934 see reference 4.
- 2- Callear, A. B., "Measurement of Energy Transfer in Molecular Collisions", Applied Optics, Supplement 2, 1965. pp 164-168.
- 3- Anderson, R. A. and R. H. McFarland, Phys. Rev., 119, 693-700, 1960.
Anderson, R. A., "The Effects of Added Gases on the Intensities of Thallium Sensitized Fluorescence", Ph.D. Dissertation, Kansas State University, 1959.
- 4- Mitchell, A. G. C. and M. W. Zemansky, "Resonance Radiation and Excited Atoms", Cambridge University Press, 1961, p. 155.
- 5- Hasted, J. B., "The Physics of Atomic Collisions", Butterworths, Washington, 1964, p. 452.
- 6- This process violates Winan's partial J sum rule. Winans, J., Rev. Mod. Phys., 16, 175-181, 1944.
- 7- Measurements of τ_{20}^a are reviewed in reference 4, pp. 123-126.
- 8- Model 11SC-1, without hand.e, Ultra-Violet Products, San Gabriel, California.
- 9- Kelley, K. K., U. S. Bureau of Mines Bulletin, 383, 1-132, 1935.
- 10- Reference 2, p. 161 and p. 167, and reference 5, p. 461.

Figure and Table Legends

Figure 1. Schematic energy level diagram indicating processes of interest. Circles represent collision processes.

Figure 2. Experimental arrangement.

C - cell

F - 2537A filter

L - mercury lamp

M_1, M_2 - monochromators

MA - ceramic mask

MF - main furnace

PM_1, PM_2, PM_3 - photomultipliers

SAF - side arm furnace

Figure 3. Resonance fluorescence and line absorption from a cell containing pure mercury vapor. The vertical bars indicate the extreme range of the measurements for three independent measurements.

Figure 4. Resonance fluorescence and line absorption from a cell containing a mercury-thallium vapor mixture. The points are average values for three measurements or calculations and have an uncertainty of ± 0.3 units. The curve marked C is found by the use of Fig. 3 and the value of the percent absorption of the cell from curve A. Curve C is corrected for the difference in cell window transmission by a constant factor determined at a thallium atom number density of about 10^{14} atoms/cm³.

Table I. Experimentally determined values of the dp-excitation cross section σ_d of thallium for the 6^3P_1 state of mercury.

Table I

Experimentally Determined Values of the De-excitation Cross Section
 σ_d of Thallium for the 6^3P_1 State of Mercury

Cell	Temperature	n_a ($\times 10^{-12}$)	n_b ($\times 10^{-12}$)	I_a^{20}/I_0	I_b^{20}/I_0	$(I_a^{20} - I_b^{20})/I_a^{20}$	Uncertainty in $(I_a^{20} - I_b^{20})/I_a^{20}$	σ_d
A	800±6°C	9	2700	10.3±0.3	11.1±0.3	0.78	±53%	16.5 ±12.0A ²
B	805±6°C	10	2300	11.8±0.3	13.7±0.3	0.161	±24%	44.5 ±16.0A ²
C	800±6°C	11	2300	13.6±0.3	15.5±0.3	0.140	±23%	38.7 ±13.6A ²
D	805±6°C	11	2900	12.6±0.3	14.9±0.3	0.182	±19%	40.0 ±12.9A ²
E	800±6°C	12	2600	14.4±0.3	16.0±0.3	0.111	±27%	27.2 ±10.6A ²
								Ave. 34 ± 13A ²
A	850±6°C	8.5	5800	9.3±0.3	11.2±0.3	0.258	±20%	27.5 ± 8.8A ²
B	860±6°C	10	6200	11.0±0.3	13.8±0.3	0.254	±17%	25.4 ± 8.8A ²
C	855±6°C	12	4800	12.2±0.3	16.1±0.3	0.320	±12%	41.2 ± 9.9A ²
D	855±6°C	12	7700	11.2±0.3	15.7±0.3	0.402	±12%	32.4 ± 7.8A ²
E	850±6°C	13	6200	13.1±0.3	16.7±0.3	0.275	±13%	27.4 ± 6.9A ²
								Ave. 31 ± 8 A ²
A	890±6°C	9.5	14000	7.6±0.3	13.2±0.3	0.736	±11%	34.2 ± 7.5A ²
B	900±6°C	10	16000	9.8±0.3	13.7±0.3	0.308	±13%	14.7 ± 3.7A ²
C	900±6°C	13	15000	10.3±0.3	17.2±0.3	0.670	± 9%	27.0 ± 5.7A ²
D	900±6°C	13	16000	9.8±0.3	17.1±0.3	0.745	± 8%	28.2 ± 5.6A ²
E	890±6°C	14	15000	11.3±0.3	17.6±0.3	0.557	± 9%	22.4 ± 4.7A ²
								Ave. 25 ± 6 A ²

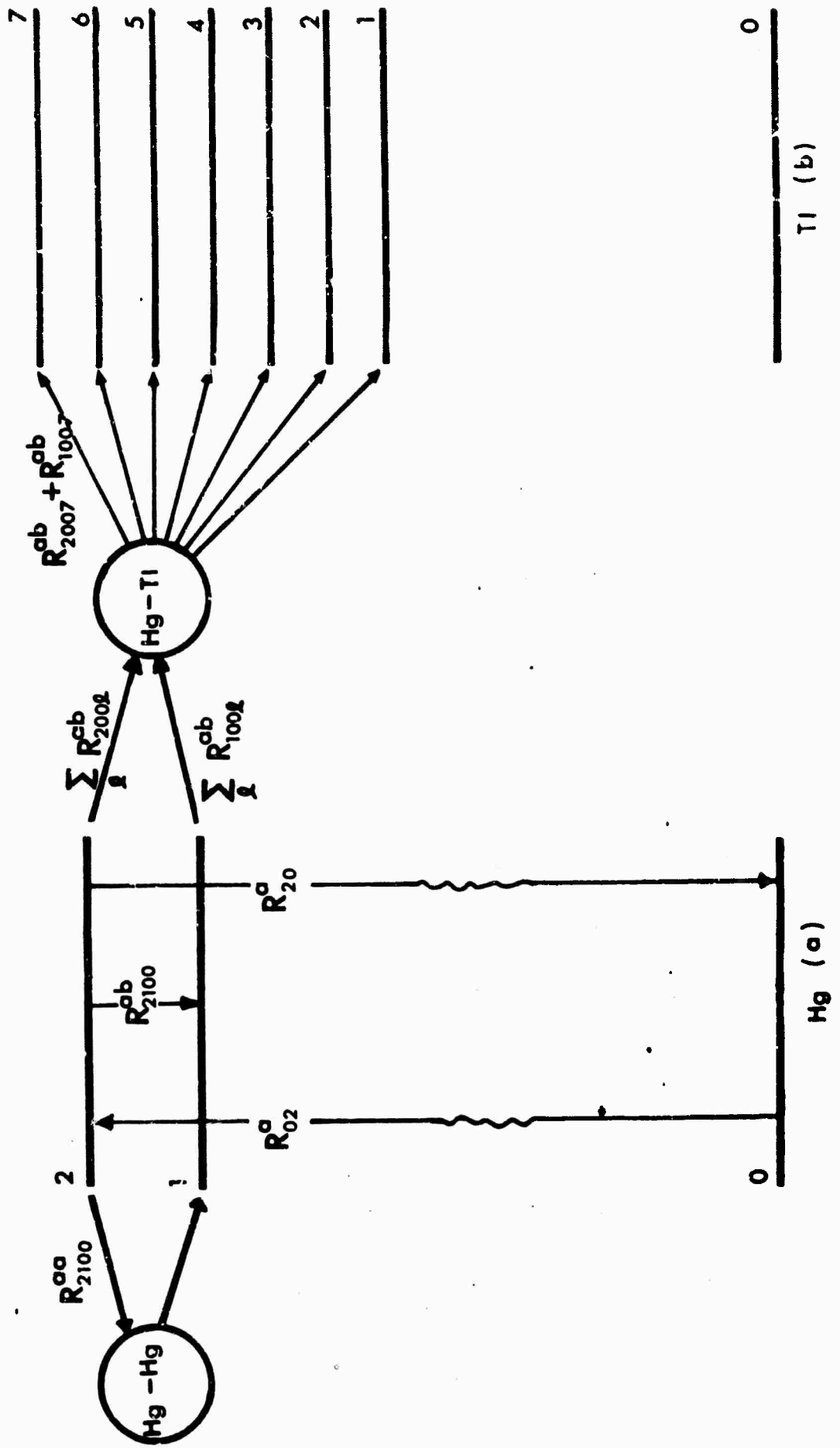


Figure 1

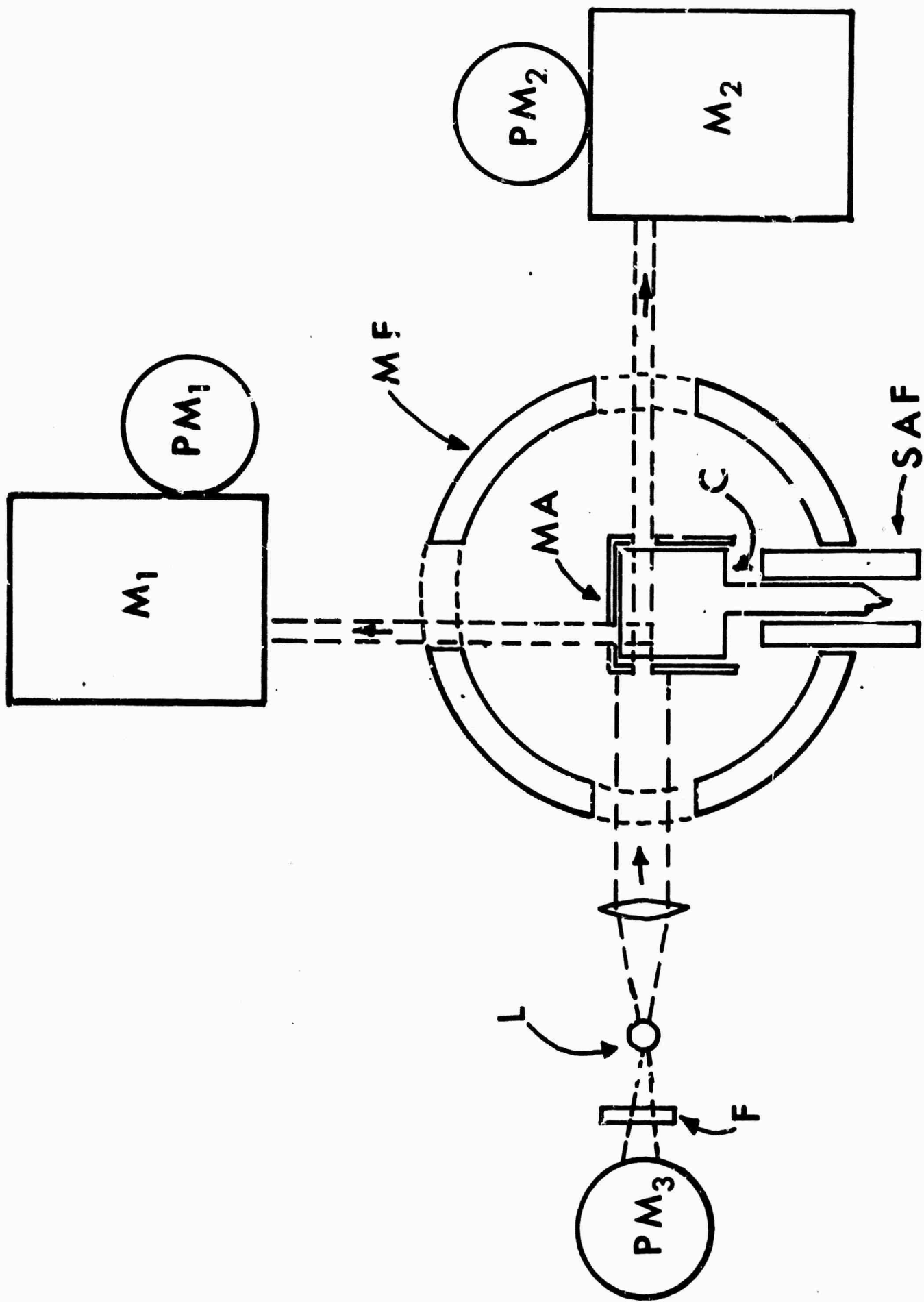


Figure 2

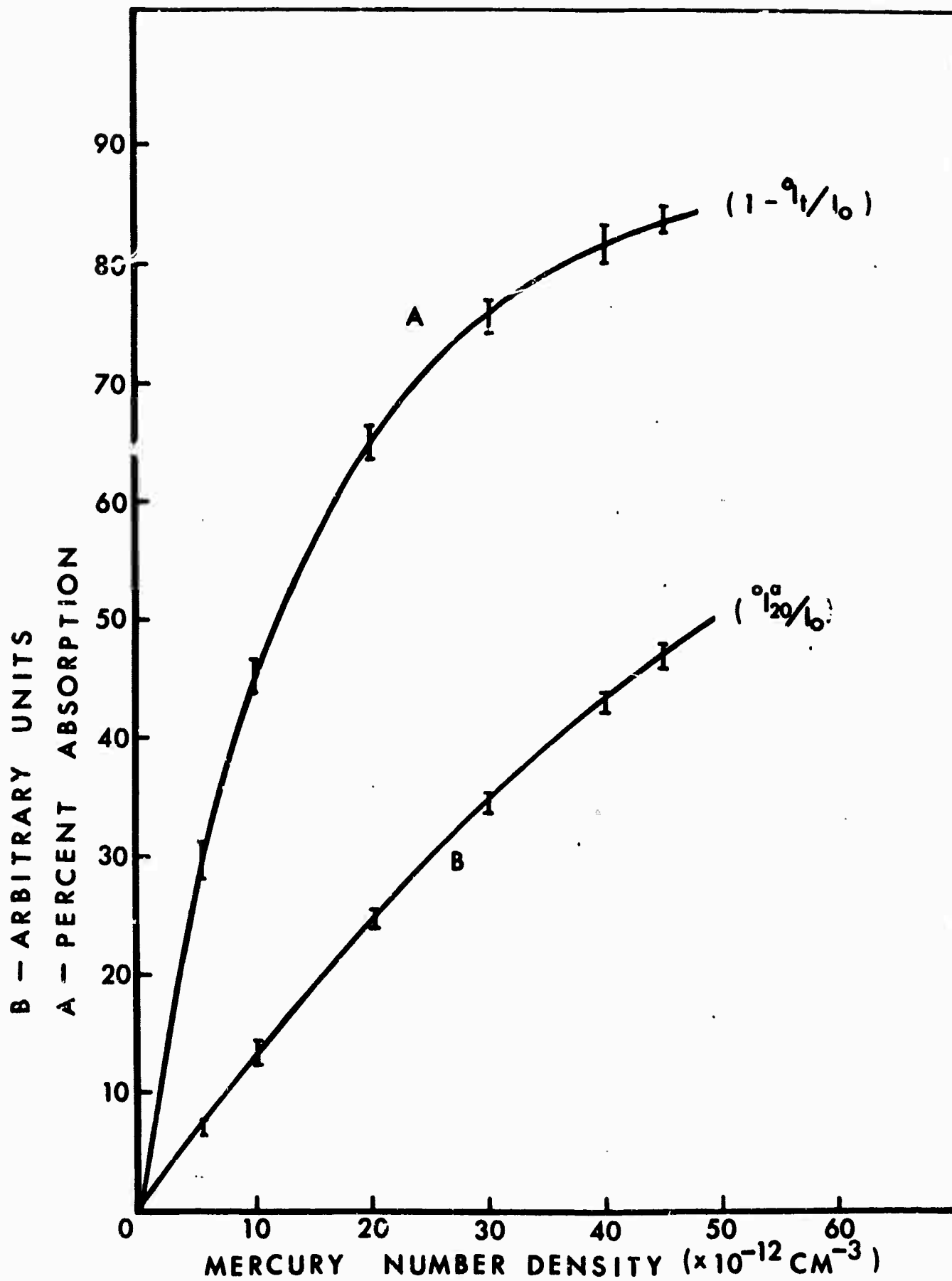


Figure 3

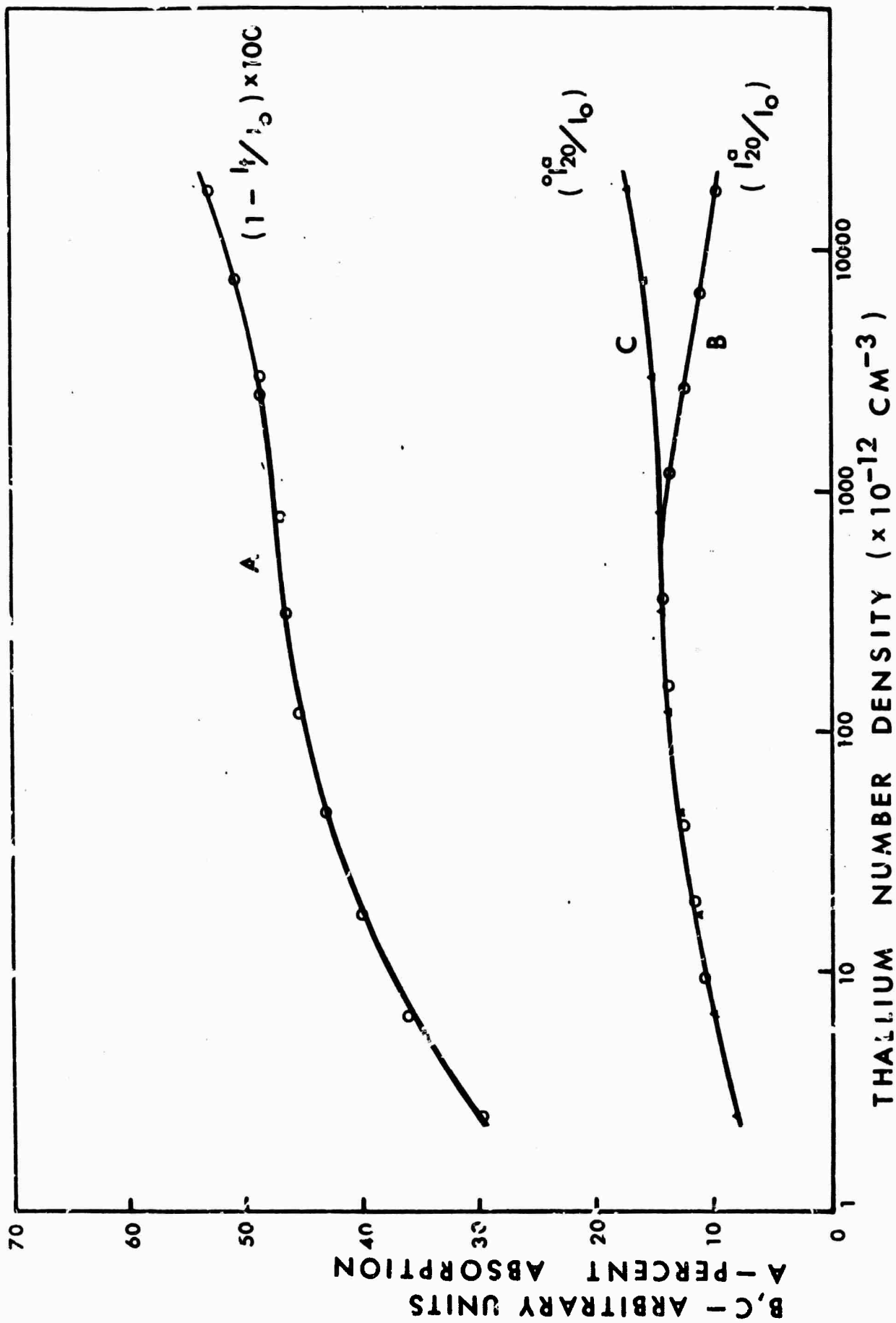


Figure 4

APPENDIX II

Experimental Determination of the Excitation Transfer Cross Section From the 6^3P_1 and 6^3P_0 States of Mercury to Thallium* (to be submitted for publication)

B. C. Hudson** and B. Curnutte, Jr.
Department of Physics, Kansas State University
Manhattan, Kansas

Abstract

The excitation transfer cross section to several of the excited states of thallium from the 6^3P_1 and 6^3P_0 states of mercury have been obtained over a range of temperatures of 800°C to 900°C. Analysis of the equilibrium rates of absorption, emission and collision processes allows the calculation of excitation transfer cross sections from experimentally determined intensity ratios of thallium sensitized fluorescence lines to the intensity of mercury resonance fluorescence, and calculated values of the thallium transition probabilities. The values obtained for the excitation transfer cross sections are comparable in magnitude with collision cross sections based on considerations of gas kinetics.

*This research is supported in part by the Office of Naval Research and the Advanced Research Projects Agency and is part of project DEFENDER.

**Present address: Lawrence Radiation Laboratories, Livermore, California

INTRODUCTION

Although the phenomenon of sensitized fluorescence has been observed for a number of years, excitation transfer cross sections for the elements involved have been measured only for sodium-mercury collisions⁽¹⁾. Equations relating the effective cross section to the number densities of the states involved (including cascade transitions) but not including wall losses) have been given by Frisch and Kraulinya⁽²⁾ and have been applied by Anderson and MacFarland⁽³⁾ to obtain relative excitation transfer cross sections for thallium sensitized fluorescence in the presence of mercury. In a previous paper⁽⁴⁾ hereafter called HCI, we have given the de-excitation cross section of thallium for the mercury 6^3P_1 state by relative intensity measurements of resonance fluorescence. In this paper we give the experimentally determined excitation transfer cross sections from mercury to several excited thallium states.

ANALYSIS

The analysis of the de-excitation of the mercury 6^3P_1 state has been given in HCI. In deriving the equations from which the excitation transfer cross sections can be determined we adopt the same notation as was used in HCI. The mercury 6^1S_0 , 6^3P_0 and 6^3P_1 states are represented by the indices 0, 1, and 2, respectively, and the thallium $6^2P_{1/2}$, $6^2P_{3/2}$, $7^2S_{1/2}$, $7^2P_{1/2}$, $7^2P_{3/2}$, $6^2D_{3/2}$, $6^2D_{5/2}$ and $8^2S_{1/2}$ states are represented by the indices 0, 1, 2, 3, 4, 5, 6 and 7, respectively. When irradiated with 2537A mercury resonance radiation, mercury atoms in a mixture of mercury and thallium vapor may absorb radiation and be raised to the 6^3P_1 state. These excited atoms may leave the excited state by sponta-

neous emission of 2537A radiation or by a radiationless transition resulting from a collision.

In treating the phenomena involved, it is desirable to adopt the following simple notation for the rates (number per unit volume per unit time) for various processes:

- (1) R_{ij}^a is the rate of an emission or absorption process by which Hg atoms are transferred from state i to state j .
- (2) R_{kl}^b is the rate of an emission or absorption process by which Tl atoms are transferred from state k to state l .
- (3) $R_{ij\ k\ l}^{ab}$ is the rate of a process involving collisions between Hg and Tl atoms in which the initial and final states of the Hg are i and j and the initial and final states of the Tl are k and l .
- (4) R_{ijpq}^{aa} is the rate of a process involving collisions between Hg atoms in which the initial and final states for one Hg atom are i and j while the initial and final states for the other Hg atom are p and q .
- (5) R_{ij}^{aw} is the rate for a process involving collisions of Hg atoms with the walls in which the initial and final states of the Hg atom are i and j .

The rate of spontaneous emission of radiation from atomic species in which the initial state is i and the final state is j is given by,

$$R_{ij}^c = n_i^c A_{ij}^c \quad (1)$$

where n_i^c is the number density of atoms of species c in state i and A_{ij}^c is the spontaneous transition probability for atoms of species c from state i to state j . A collision transfer rate is given by an equation of the form,

$$R_{ij,kl}^{ab} = n_i^a n_k^b v_{20}^{ab} \sigma_{ij,kl}^{ab} \quad (2)$$

where, $\sigma_{ij,kl}^{ab}$ is the collision cross section⁽⁵⁾ for this process and n_i^a is the number density of atom of species a in state i, n_k^b is the number density of atoms of species b in state k, and

$$v_{20}^{ab} = [8\pi RT(1/M_a + 1/M_b)]^{1/2} \quad \text{is a} \quad (3)$$

quantity proportional to the relative velocity of collision of the atoms involved in the collision.

The equations for the equilibrium of the excited (6^3P_1) state of mercury have been discussed in HCI. The rate equations for the equilibrium of the remaining states of the system are:

(a) For the 6^3P_0 state of mercury

$$R_{2100}^{ab} + R_{2100}^{aa} = R_{10}^a + \sum_{j=1}^7 R_{100j}^{ab} + R_{10}^{aw} \quad (4)$$

with R_{10}^{aw} representing the rate of loss of metastable mercury atoms in collision with the walls.

(b) For the $8^2S_{1/2}$ state of thallium,

$$R_{2007}^{ab} + R_{1007}^{ab} = R_{70}^b + R_{71}^b + R_{73}^b + R_{74}^b \quad (5)$$

(c) For the $6^2D_{5/2}$ state of thallium,

$$R_{2006}^{ab} + R_{1006}^{ab} = R_{60}^b + R_{64}^b \quad (6)$$

(d) For the $6^2D_{3/2}$ state of thallium,

$$R_{2005}^{ab} + R_{1005}^{ab} = R_{50}^b + R_{51}^b + R_{53}^b + R_{54}^b \quad (7)$$

(e) For the $7^2P_{3/2}$ state of thallium,

$$R_{2004}^{ab} + R_{1004}^{ab} = R_{42}^b - R_{54}^b - R_{74}^b - R_{64}^b \quad (8)$$

(f) For the $7^2P_{1/2}$ state of thallium

$$R_{2003}^{ab} + R_{1003}^{ab} = R_{32}^b - R_{53}^b - R_{73}^b \quad (9)$$

and (g) For the $7^2S_{1/2}$ state of thallium,

$$R_{2002}^{ab} + R_{1002}^{ab} = R_{20}^b + R_{21}^b - R_{42}^b \cdot R_{32}^b \quad (10)$$

These rate equations are written with the assumption that cascade transitions from states higher than the $8^2S_{1/2}$ state of thallium are negligible, and assumption which seems justified since for conditions of the experiment reported here no radiation⁽⁶⁾ from higher thallium states was observed.

If I_{ij}^a represents the output voltage from the detector amplifier when all of the radiation within the acceptance angle of the monochromator of the doppler broadened line emitted by the spontaneous transition of atoms of species a from state i to state j is detected then,

$$I_{ij}^a = K_{ij}^a K_g n_i^a A_{ij}^a h\nu_{ij}^a \quad (11)$$

where, K_{ij}^a is the efficiency of the detector system for radiation of frequency ν_{ij}^a , K_g is a constant depending on the geometry of the experiment, and ν_{ij}^a is the central frequency of the spectral line emitted by an atom of species a in the transition from state i to state j.

Equation (11) can be rewritten in the form,

$$n_i^a = (I_{ij}^a \lambda_{ij}^a) / (hc K_g K_{ij}^a A_{ij}^a) \quad (12)$$

from which all number densities in the rate equations can be replaced by measurable quantities or quantities which may be calculated from

theory. Using equation 10 of HCI and Equations 1, 2, 3, and 12 we can solve the rate equations for the sums of the excitation transfer cross-sections from the excited and metastable mercury states and obtain the following equations:

$$\left(\frac{I_{20}^a - I_{20}^a}{I_{20}^a} \right) \frac{\lambda_{20}^a}{K_{20}^a} = \frac{I_{21}^b \lambda_{21}^b}{I_{20}^a K_{21}^b} + \frac{I_{51}^b \lambda_{51}^b}{I_{20}^a K_{51}^b} + \frac{I_{61}^b \lambda_{61}^b}{I_{20}^a K_{61}^b} + \frac{I_{71}^b \lambda_{71}^b}{I_{20}^a K_{71}^b} + \frac{\lambda_{20}^a R_{10}^{aw}}{K_{20}^a A_{20}^a n_2^a} \quad (13)$$

$$\sigma_{2007}^{ab} + \frac{n_1^a}{n_2^a} \sigma_{1007}^{ab} = \frac{I_{71}^b \lambda_{71}^b}{K_{71}^b} \left(1 + \frac{A_{70}^b}{A_{71}^b} + \frac{A_{73}^b}{A_{71}^b} + \frac{A_{74}^b}{A_{71}^b} \right) \times \frac{A_{20}^a K_{20}^a}{I_{20}^a \lambda_{20}^a n_0^b v_{20}^{ab}} \quad (14)$$

$$\sigma_{2006}^{ab} + \frac{n_1^a}{n_2^a} \sigma_{1006}^{ab} = \frac{I_{61}^b \lambda_{61}^b}{K_{61}^b} \left(1 + \frac{A_{64}^b}{A_{61}^b} \right) \frac{A_{20}^a K_{20}^a}{I_{20}^a \lambda_{20}^a n_0^b v_{20}^{ab}} \quad (15)$$

$$\sigma_{2005}^{ab} + \frac{n_1^a}{n_2^a} \sigma_{1005}^{ab} = \frac{I_{51}^b \lambda_{51}^b}{K_{51}^b} \left(1 + \frac{A_{50}^b}{A_{51}^b} + \frac{A_{53}^b}{A_{51}^b} + \frac{A_{54}^b}{A_{51}^b} \right) \times \frac{A_{20}^a K_{20}^a}{I_{20}^a \lambda_{20}^a n_0^b v_{20}^{ab}} \quad (16)$$

$$\sigma_{2004}^{ab} + \frac{n_1^a}{n_2^a} \sigma_{2004}^{ab} = \left(\frac{I_{42}^b \lambda_{42}^b}{K_{42}^b} - \frac{I_{54}^b \lambda_{54}^b}{K_{54}^b} - \frac{I_{64}^b \lambda_{64}^b}{K_{64}^b} - \frac{I_{74}^b \lambda_{74}^b}{K_{74}^b} \right) \times \frac{A_{20}^a K_{20}^a}{I_{20}^a \lambda_{20}^a n_0^b v_{20}^{ab}} \quad (17)$$

$$\sigma_{2003}^{ab} + \frac{n_1^a}{n_2^a} \sigma_{1003}^{ab} = \left(\frac{I_{32}^b \lambda_{32}^b}{K_{32}^b} - \frac{I_{53}^b \lambda_{53}^b}{K_{53}^b} - \frac{I_{73}^b \lambda_{73}^b}{K_{73}^b} \right) \times \frac{A_{20}^a K_{20}^a}{I_{20}^a \lambda_{20}^a n_0^b v_{20}^{ab}} \quad (18)$$

$$\sigma_{2002}^{ab} + \frac{n_1^a}{n_2^a} \sigma_{1002}^{ab} = \left(\frac{I_{21}^b \lambda_{21}^b}{K_{21}^b} \left(1 + \frac{A_{20}^b}{A_{21}^b} \right) - \frac{I_{42}^b \lambda_{42}^b}{K_{42}^b} - \frac{I_{32}^b \lambda_{32}^b}{K_{32}^b} \right) \times \frac{A_{20}^a K_{20}^a}{I_{20}^a \lambda_{20}^a n_0^b v_{20}^{ab}} \quad (19)$$

$$\frac{A_{20}^a K_{20}^a}{I_{20}^a \lambda_{20}^a n_0^b v_{20}^{ab}}$$

In the above equations the losses at the walls have been omitted in all but equation 13 because of the short radiative lifetimes of the states involved.

The quantities which appear in equations (13-19) are not all measurable. Because the lines from the $6^2D_{5/2}$ and $6^2D_{3/2}$ are doppler broadened and overlap, intensities of lines originating at these levels cannot be separately determined. Hence, equations 15 and 16 are added to obtain the equation,

$$\left(\frac{A_{61}^b}{A_{61}^b + A_{64}^b} \right) \left(\sigma_{2006}^{ab} + \frac{n_1^a}{n_2^a} \sigma_{1006}^{ab} \right) + \left(\frac{A_{51}^b}{A_{51}^b + A_{53}^b + A_{54}^b} \right) \left(\sigma_{2005}^{ab} + \frac{n_1^a}{n_2^a} \sigma_{1005}^{ab} \right) = \left(\frac{I_{61}^b + I_{51}^b}{I_{20}^a} \right) \frac{\lambda_{61}^b}{\lambda_{20}^a} \frac{K_{20}^a}{K_{61}^b} \frac{A_{20}^a}{n_0^b v_{20}^{ab}} \quad (20)$$

Assuming that the energy differences between the 6^3P_1 and 6^3P_0 states of mercury and the $7^2S_{1/2}$ state of thallium are so large that the cross-sections for transfer to the thallium $7^2S_{1/2}$ state are negligible we can use equation 19 to eliminate the unmeasurable intensities I_{42}^b and I_{32}^b from equations 17 and 18. This procedure yields the equation,

$$\begin{aligned}
 (\sigma_{2004}^{ab} + \sigma_{2003}^{ab}) + \frac{n_1^a}{n_2} (\sigma_{1004}^{ab} + \sigma_{1003}^{ab}) &= \left(\frac{I_{21}^b}{I_{20}^a} \frac{\lambda_{21}^b}{\lambda_{20}^a} \frac{K_{20}^a}{K_{21}^b} \right. \\
 &- \frac{I_{51}^b}{I_{20}^a} \frac{\lambda_{51}^b}{\lambda_{20}^a} \frac{K_{20}^a}{K_{51}^b} \left(\frac{A_{53}^b + A_{54}^b}{A_{51}^b} \right) - \frac{I_{61}^b}{I_{20}^a} \frac{\lambda_{61}^b}{\lambda_{20}^a} \frac{K_{20}^a}{K_{61}^b} \frac{A_{64}^b}{A_{61}^b} - \frac{I_{71}^b}{I_{20}^a} \frac{\lambda_{71}^b}{\lambda_{20}^a} \frac{K_{20}^a}{K_{71}^b} \times \\
 &\left. \left(\frac{A_{73}^b + A_{74}^b}{A_{71}^b} \right) \right) \frac{A_{20}^a}{n_0 v_{20}^{ab}} .
 \end{aligned} \tag{21}$$

Equation 14 may be rewritten as,

$$\sigma_{2007}^{ab} + \frac{n_1^a}{n_2} \sigma_{1007}^{ab} = \frac{I_{71}^b}{I_{20}^a} \frac{\lambda_{71}^b}{\lambda_{20}^a} \frac{K_{20}^a}{K_{71}^b} \frac{A_{20}^a}{n_0 v_{20}^{ab}} . \tag{22}$$

For the number densities of ground state thallium atoms which will be encountered in the experiment, 10^{15} - 10^{18} cm^{-3} , the resonance radiation of thallium will be imprisoned. No thallium resonance radiation was observed from the cell, thus the combined effect of the imprisonment of resonance radiation and competing modes of de-excitation yield an effective zero transition probability for the radiative transitions to the ground state. Hence, in equations 20, 21, and 22, the spontaneous transition probabilities A_{20}^b are set equal to zero.

The notation of equations 20, 21, and 22 can be somewhat simplified by defining the following composite cross sections,

$$\sigma_{34d} = (\sigma_{2004}^{ab} + \sigma_{2003}^{ab}) + \frac{n_1^a}{n_2} (\sigma_{1004}^{ab} + \sigma_{1003}^{ab}) \quad (23)$$

$$\sigma_{56d} = (\sigma_{2006}^{ab} + \sigma_{2005}^{ab}) + \frac{n_1^a}{n_2} (\sigma_{1006}^{ab} + \sigma_{1005}^{ab}) \quad (24)$$

$$\sigma_{7d} = \sigma_{2007}^{ab} + \frac{n_1^a}{n_2} \sigma_{1007}^{ab} \quad (25)$$

These cross sections are similar to what Frisch and Kraulinia call effective cross sections since they are defined for processes involving collisions of thallium with mercury atoms in the 6^3P_1 and 6^3P_0 states. These three cross sections can be determined from measurements of the relative intensities of the sensitized fluorescence lines of thallium to the 2537A resonance fluorescence line of mercury, measurement of the relative sensitivity of the detection system for sensitized fluorescence lines of thallium to the resonance fluorescence line of mercury, and calculation of the transition probabilities between the various states of thallium.

Experimental

The experimental arrangement used for the measurements was the same as that used for the measurement of mercury resonance fluorescence reported in HCl. Four independent sets of intensity readings were taken

on one cell, cell D of HCl. In addition to the intensity of mercury resonance fluorescence the intensities of the 3230A, 3519-29A, and 5350A sensitized fluorescence lines of thallium were also measured.

The results of the intensity measurements are given in Table 1. The first column of Table 1 shows the wavelength of the thallium radiation being measured. The second column shows the reading of the photomultiplier readout amplifier recorder for the thallium sensitized fluorescence radiation. The uncertainty in the reading of the photomultiplier readout amplifier recorder was ± 0.5 units. The third column gives the reading of the photomultiplier readout amplifier recorder for the mercury 2537A resonance fluorescence. The monochromator and slit system was maintained at the same geometry for the measurements shown in columns two and three. The fourth column gives the ratio of the second and third columns. The fifth column gives the ground state thallium atom number density as determined from the temperature of the side arm of the cell with ideal gas law correction for the temperature of the main body of the cell. The uncertainty in the ground state number density of thallium atoms is $\pm 12\%$ because of uncertainty of temperature measurement. The sixth column shows the temperature of the main body of the cell where the collisions of interest are taking place. The last column gives the percent uncertainty in the ratio recorded in column four.

In our previous measurements the relative intensities of mercury resonance fluorescence with and without thallium present was not dependent on the spectral sensitivity of the monochromators and detecting systems. However, the measurement of the relative intensity of the thallium line fluorescence to the mercury resonance fluorescence requires a knowledge of the relative sensitivity of the monochromator and detecting system. In order to determine the relative sensitivity of the monochromator and

detection system was used a Hanovia low-pressure mercury arc and a 250 mm, Bausch and Lomb grating monochromator as a source of nearly monochromatic radiation for the 2537, 3012, 3131, 3341, 3650, 4358, and 5450A lines of mercury. The slits of this monochromator were kept narrow so that all radiation in the spectral band pass of the source monochromator would be transmitted by the measuring monochromator. A Reeder thermopile with a quartz window designed for use on the ultraviolet region was employed to determine the relative radiant flux incident on the slit of the monochromator which was used for all the fluorescence measurements. The response of the photomultiplier, amplifier and the thermopile EMF were recorded for each of the wavelengths involved. The thermopile was masked with apertures to receive the same incident radiation over the same area and at the same acceptance angle as the monochromator. In making the calibration, the thermopile was assumed to have a flat response within $\pm 10\%$ over the spectral range 2500A to 5500A. This assumption was based on Christensen and Ames⁽¹⁷⁾ results on a similar thermopile. The results of these measurements are given in Table 2.

The first column of Table 2 gives the wavelength of the radiation being used for the measurement. The second column tabulates the voltage on the photomultiplier. The 1 P 28 photomultiplier used has a glass envelope and the efficiency of the photomultiplier is greatly reduced for 2537A radiation as compared to the efficiency for the detection of radiation of the other wavelengths involved. In order to keep the output of the photomultiplier readout recorder on scale the voltage on the photomultiplier was increased for the measurement of the 2537A radiation. The ratio of the readings of the photomultiplier readout amplifier was experimentally determined to be 44.2 when the photomultiplier

voltage was increased from 350V to 500V. The third column lists the reading on the photomultiplier readout amplifier recorder. The fourth column shows the value of column three corrected for the reduction of the photomultiplier voltage below 500V. The fifth column shows the output voltage of the thermopile for the same incident flux as was present at the entrance slit of the measuring monochromator. The sixth column lists the ratio of the readings of columns four to five. The seventh column gives the average percentage deviation in the values of column six to the average of the values in column six for each wavelength. Column eight tabulates the relative efficiency of the monochromator detector system for 2537A radiation to the radiation of the wavelength given in column one.

The extrapolated values of the relative response of the monochromator-detector system at the wavelength of the thallium sensitized fluorescence lines are also shown in the lower part of Table 2. The extrapolated values were determined by passing a smooth curve through the points determined by the measurements and finding the relative response from the ordinate of the curve at the wavelengths of the thallium lines under study. These measurements showed an average deviation of less than 4%, however, the relative response was assigned a 10% uncertainty because of the variation in Christensen and Ames' results on several thermopiles.

The transition probabilities for the various thallium transitions were calculated by the method of Bates and Damgaard⁽⁸⁾ and are tabulated in Table 3. Bates and Damgaard compared calculated transition probabilities for several thallium transitions with measured lifetimes and found the agreement with experimental values to be within the experimental error. Only ratios of transition probabilities are used in the determination of the excitation exchange cross sections and a 10% uncertainty

was assigned to these ratios. The value of A_{20}^a corresponding to Garrett's⁽¹⁰⁾ measured value of 1.08×10^{-7} sec for the lifetime of the 6^3P_1 state in mercury was used in evaluating the excitation exchange cross section. This value of A_{20}^a has a 5% uncertainty. The number densities of mercury and thallium atoms were determined in the same manner and with the same accuracy as was described in HCl.

Using the measured intensity ratios of Table I, the measured relative response of the monochromator detector system from Table 2, and the computed transition probabilities from Table 3, one can calculate the excitation-transfer cross sections from the mercury 5^3P_1 (2) and 6^3P_0 (1) states to the thallium $8^2S_{1/2}$ (?), 6^2D (5 and 6), and 7^2P (3 and 4) states. One can take advantage of the values of the transition probability ratios to write the following approximate equations for the cross sections of interest:

$$\sigma_{34d} = \left(\frac{I_{21}^b}{I_{20}^a} \frac{\lambda_{21}^b}{\lambda_{20}^a} \frac{K_{20}^a}{K_{21}^b} - \frac{I_{71}^b}{I_{20}^a} \frac{\lambda_{71}^b}{\lambda_{20}^a} \frac{K_{20}^a}{K_{71}^b} \frac{A_{73}^b + A_{74}^b}{A_{71}^b} \right) \frac{A_{20}^a}{n_0^b v_{20}^{ab}}, \quad (26)$$

$$\sigma_{56d} = \frac{I_{61}^b + I_{51}^b}{I_{20}^a} \frac{\lambda_{61}^b}{\lambda_{20}^a} \frac{K_{20}^a}{K_{61}^b} \frac{A_{20}^a}{n_0^b v_{20}^{ab}}, \quad (27)$$

$$\sigma_{7d} = \frac{I_{71}^b}{I_{20}^a} \frac{\lambda_{71}^b}{\lambda_{20}^a} \frac{K_{20}^a}{K_{71}^b} \frac{A_{20}^a}{n_0^b v_{20}^{ab}}. \quad (28)$$

The approximations made in equations 26-28 should cause less than 2% error in the cross sections resulting from the use of these equations. The cross sections obtained by the use of equation 26-28 and the measurements reported here are tabulated in Table 4.

There appears to be a decrease in cross sections σ_{7d} and σ_{56d} as

the temperature is increased which is in keeping with the reduction of collision time at higher temperatures. The cross section σ_{34d} , however, increases with increasing temperature. This can be accounted for by noting that the decrease of mean free path, as the thallium number density increases, reduces the rate of loss of metastable (6^3P_0) mercury atoms to the walls and that the number density of metastable mercury atoms rises at the higher temperatures. If the σ_{34d} cross section is due primarily to transfer of energy from metastable mercury atoms this increase would be accounted for by the increase of the term $\frac{n_2^a}{n_1^a} (\sigma_{1003}^{ab} + \sigma_{1004}^{ab})$ in σ_{34d} even though the cross sections σ_{1003}^{ab} and σ_{1004}^{ab} might decrease with increasing temperature. Measurements of the ratio n_2^a/n_1^a are needed to substantiate this point.

The cross sections in Table 4 are comparable with gas kinetic collision cross sections and are of the same order of magnitude as the energy transfer cross section from the helium (2^1S_0) to the neon ($3s_2$) state of $4.1A^2$.⁽¹¹⁾ Thus it would seem that the cross sections for energy transfer in the mercury-thallium system are sufficiently large for the 6D and 7P states to allow population inversion by collision pumping with the excited and metastable mercury atoms.

Acknowledgements

We are indebted to Dr. Dudley Williams for his constructive criticism of the manuscript.

Table 1

λ	I_{T1}	I_{2537}	I_{T1}/I_{2537}	b_{n0} $\times 10^{-14}$	T $^{\circ}K$	error in I_{T1}/I_{2537}
3230	1.0	24.0	.042	21.0	1073	52
	0.8	22.0	.036	24.4	1058	52
	1.0	24.0	.042	21.0	1058	52
	1.0	24.0	.042	24.0	1068	52
3519-29	9.5	22.5	.42	21.1	1069	7
	9.5	22.0	.43	24.4	1058	7
	11.0	24.5	.45	21.1	1068	7
	12.5	24.0	.52	28.2	1068	7
5350	8.5	22.5	.38	21.1	1069	10
	9.5	22.0	.43	24.4	1068	10
	11.0	24.5	.45	25.9	1058	10
	11.5	24.0	.47	25.9	1058	10
3230	1.0	21.5	.047	41.2	1115	27
	1.6	21.0	.073	41.2	1115	27
	2.0	22.0	.091	63.2	1115	27
	2.0	23.0	.087	74.4	1115	27
3519-29	19.5	21.0	.93	41.2	1115	5
	20.0	22.0	.91	33.8	1115	5
	32.0	22.0	1.45	63.7	1115	5
	34.0	23.0	1.48	63.7	1115	5
5350	19.0	21.5	.90	41.2	1115	6
	18.0	22.0	.82	41.2	1115	6
	26.8	22.0	1.22	60.3	1121	6
	35.6	23.0	1.55	74.4	1115	6
3230	3.0	22.0	.136	125	1164	17
	3.0	18.8	.180	110	1164	17
	3.0	18.5	.160	125	1164	17
3519-29	51.5	22.0	2.34	140	1164	3
	52.0	21.0	2.50	141	1158	3
	44.5	19.0	2.34	110	1164	3
	45.0	18.5	2.43	140	1164	3
5350	62.5	22.0	2.80	140	1164	4
	50.0	21.0	2.40	140	1164	4
	63.5	19.0	3.30	110	1164	4
	52.7	18.5	2.90	110	1164	4

Table 2

λ A	V Volts	I_{PM}	Corrected I_{PM}	I_{TP} μV	I_{PM}/I_{TP}	Average I_{PM}/I_{TP}	Average I_{PM}/I_{TP} deviation %	$\frac{\text{Average}(I_{PM}/I_{TP})_{2537}}{\text{Average}(I_{PM}/I_{TP})_{\lambda}}$
2537	500	40.5	40.5	6.6	6.13	6.00	4	1.00
		40.5	50.5	6.8	5.95			
		40.8	40.8	6.4	6.38			
		40.0	40.0	7.2	5.56			
3012	350	32.5	1436	9.1	158	157	0.6	.0382
		32.5	1436	9.3	155			
		31.3	1383	8.7	159			
		31.3	1383	8.8	157			
3131	350	34.2	1520	7.8	195	188	2	.0319
		33.7	1490	7.9	189			
		33.9	1500	7.8	192			
		33.9	1500	8.4	179			
3650	350	90.2	3985	9.3	429	407	4	.0147
		89.0	3935	9.5	420			
		87.4	3870	10.2	380			
		86.4	3820	9.6	398			
4358	350	56.0	2475	7.8	317	323	4	.0185
		55.5	2450	7.0	350			
		55.5	2450	8.0	306			
		54.8	2425	7.6	319			
5450	350	34.0	1504	6.5	232	228	2	.0263
		34.6	1529	6.6	232			
		35.0	1546	7.1	218			
		35.0	1546	6.7	231			
Extrapolated values								
3230	500							.0237
3519-29	500							.0178
5350	500							.0257

Table 3

Transition	A_{ij}^b ($\times 10^{-8} \text{sec}^{-1}$)
$7^2S_{1/2} - 6^2P_{1/2}$	0.217
$7^2S_{1/2} - 6^2P_{3/2}$	0.382
$7^2P_{1/2} - 7^2S_{1/2}$	0.158
$7^2P_{3/2} - 7^2S_{1/2}$	0.206
$6^2D_{3/2} - 6^2P_{3/2}$	0.200
$6^2D_{5/2} - 6^2P_{3/2}$	1.21
$6^2D_{3/2} - 6^2P_{1/2}$	1.25
$6^2D_{3/2} - 7^2P_{3/2}$	0.00008
$6^2D_{5/2} - 7^2P_{3/2}$	0.0008
$6^2D_{3/2} - 7^2P_{1/2}$	0.0043
$8^2S_{1/2} - 6^2P_{3/2}$	0.103
$8^2S_{1/2} - 6^2P_{1/2}$	0.049
$8^2S_{1/2} - 7^2P_{3/2}$	0.046
$8^2S_{1/2} - 7^2P_{1/2}$	0.033

Table 4

Temperature	σ_{7d}	σ_{56d}	σ_{34d}	σ_d
°C	A ²	A ²	A ²	A ²
800°	0.7±0.4	3.0±1.0	5.6±1.9	34±13
850°	0.5±0.2	3.6±1.1	6.6±2.1	31±8
900°	0.4±0.1	2.7±0.8	7.4±2.3	25±6

Table Legends

- Table 1. Experimentally determined values of the ratio of the response of the detector system for sensitized fluorescence lines of thallium compared to the response of the detector system for the 2537Å resonance fluorescence of mercury.
- Table 2. Experimentally determined values of the relative sensitivity of the detector system for the 2537Å resonance fluorescence of mercury compared to other mercury lines.
- Table 3. Calculated transition probabilities, calculated by the method of Bates and Damgaard⁽⁸⁾.
- Table 4. Excitation transfer cross sections from the 6^3P_1 and 6^3P_0 mercury states to the thallium $8^2S_{1/2}(\sigma_{7d})$, $6^2P_{5/2, 3/2}(\sigma_{5, 6d})$ and $7^2P_{3/2, 1/2}(\sigma_{3, 4d})$ states.

- 1- Kraulinya, E. K., Opt. i Spektroskopiya, 17, 466, 1964.
Rautian, S. G. and A. S. Khaikin, Opt. i Spektroskopiya, 18, 406, 1965.
Nikitin, E. E. and V. K. Bykhovskii, Opt. i Spektroskopiya, 17, 809, 1964.
- 2- Frish, S. E. and E. K. Kraulinya, Dokl. Akad. Nauk SSSR, 101, 837, 1955.
- 3- Anderson, R. A. and R. H. McFarland, Phys. Rev. 119, 693, 1960.
- 4- Appendix I, this report.
- 5- Mitchell, A. G. C. and M. W. Zemansky, "Resonance Radiation and Excited Atoms", Cambridge University Press, 1961, p. 155.
For alternative definition of cross section see, Hasted, J. B., "The Physics of Atomic Collisions", Butterworths, Washington, 1964, p. 452.
- 6- Frish, S. E. and O. P. Bochkova, J. Exptl. Theoret. Phys. (USSR) 43, 331, 1962.
- 7- Christensen, R. L. and I. Ames, J. Opt. Soc. Amer. 51, 224, 1961.
- 8- Bates, D. R. and A. Damgaard, Phil. Trans. A242, 101, 1949.
- 9- Callear, A. B., "Measurement of Energy Transfer in Molecular Collisions", Applied Optics, Supplement 2, 1965, pp 164-168.
- 10- Mitchell, A. G. C. and M. W. Zemansky, "Resonance Radiation and Excited Atoms" Cambridge University Press, 1961, pp 123-126.
- 11- Benton, E. E., F. A. Matson, E. E. Ferguson, and W. W. Roberts, Phys. Rev. 128, 206, 1962.

DOCUMENT CONTROL DATA - R&D

(Security classification of title, body of abstract and indexing annotation must be entered when the overall report is classified)

1. ORIGINATING ACTIVITY (Corporate author)		2a. REPORT SECURITY CLASSIFICATION	
Kansas State University		Unclassified	
		2b. GROUP	
3. REPORT TITLE			
Sensitized Fluorescence			
4. DESCRIPTIVE NOTES (Type of report and inclusive dates)			
Final Report (1 April 1963 - 31 December 1965)			
5. AUTHOR(S) (Last name, first name, initial)			
Curnutte, Basil, Jr.			
6. REPORT DATE		7a. TOTAL NO. OF PAGES	7b. NO. OF REFS
31 December, 1965		45	28
8a. CONTRACT OR GRANT NO.		9a. ORIGINATOR'S REPORT NUMBER(S)	
3634(02)			
a. PROJECT NO.			
c.		9b. OTHER REPORT NO(S) (Any other numbers that may be assigned this report)	
d.			
10. AVAILABILITY/LIMITATION NOTICES			
11. SUPPLEMENTARY NOTES		12. SPONSORING MILITARY ACTIVITY	
		Office of Naval Research Department of the Navy Washington, D. C. 20360	
13. ABSTRACT			
<p>The quenching of mercury resonance fluorescence by thallium in a mercury thallium vapor mixture has been measured to determine the quenching cross section of thallium for the 6^3P_1 state of mercury. The results for the quenching cross section at 800°C, 850°C and 900°C are given.</p> <p>The cross section for the transfer of energy to several of the thallium excited states on collision with excited and metastable mercury atoms were determined by measurements of the relative intensities of thallium sensitized fluorescence radiation to mercury resonance fluorescence radiation. The excitation transfer cross sections as determined from the measurements are reported.</p> <p>The implications of the magnitudes of the energy transfer cross sections on the prospects for the use of a mercury-thallium vapor in a laser system are discussed.</p>			

14. KEY WORDS	LINK A		LINK B		LINK C	
	ROLE	WT	ROLE	WT	ROLE	WT
Sensitized Fluorescence						
Quenching						
Excitation Transfer						
Collision Cross Sections						

INSTRUCTIONS

1. ORIGINATING ACTIVITY: Enter the name and address of the contractor, subcontractor, grantee, Department of Defense activity or other organization (corporate author) issuing the report.

2a. REPORT SECURITY CLASSIFICATION: Enter the overall security classification of the report. Indicate whether "Restricted Data" is included. Marking is to be in accordance with appropriate security regulations.

2b. GROUP: Automatic downgrading is specified in DoD Directive 5200.10 and Armed Forces Industrial Manual. Enter the group number. Also, when applicable, show that optional markings have been used for Group 3 and Group 4 as authorized.

3. REPORT TITLE: Enter the complete report title in all capital letters. Titles in all cases should be unclassified. If a meaningful title cannot be selected without classification, show title classification in all capitals in parentheses immediately following the title.

4. DESCRIPTIVE NOTES: If appropriate, enter the type of report, e.g., interim, progress, summary, annual, or final. Give the inclusive dates when a specific reporting period is covered.

5. AUTHOR(S): Enter the name(s) of author(s) as shown on or in the report. Enter last name, first name, middle initial. If military, show rank and branch of service. The name of the principal author is an absolute minimum requirement.

6. REPORT DATE: Enter the date of the report as day, month, year, or month, year. If more than one date appears on the report, use date of publication.

7a. TOTAL NUMBER OF PAGES: The total page count should follow normal pagination procedures, i.e., enter the number of pages containing information.

7b. NUMBER OF REFERENCES: Enter the total number of references cited in the report.

8a. CONTRACT OR GRANT NUMBER: If appropriate, enter the applicable number of the contract or grant under which the report was written.

8b, 8c, & 8d. PROJECT NUMBER: Enter the appropriate military department identification, such as project number, subproject number, system numbers, task number, etc.

9a. ORIGINATOR'S REPORT NUMBER(S): Enter the official report number by which the document will be identified and controlled by the originating activity. This number must be unique to this report.

9b. OTHER REPORT NUMBER(S): If the report has been assigned any other report numbers (other by the originator or by the sponsor), also enter this number(s).

10. AVAILABILITY/LIMITATION NOTICES: Enter any limitations on further dissemination of the report, other than those

imposed by security classification, using standard statements such as:

- (1) "Qualified requesters may obtain copies of this report from DDC."
- (2) "Foreign announcement and dissemination of this report by DDC is not authorized."
- (3) "U. S. Government agencies may obtain copies of this report directly from DDC. Other qualified DDC users shall request through _____."
- (4) "U. S. military agencies may obtain copies of this report directly from DDC. Other qualified users shall request through _____."
- (5) "All distribution of this report is controlled. Qualified DDC users shall request through _____."

If the report has been furnished to the Office of Technical Services, Department of Commerce, for sale to the public, indicate this fact and enter the price, if known.

11. SUPPLEMENTARY NOTES: Use for additional explanatory notes.

12. SPONSORING MILITARY ACTIVITY: Enter the name of the departmental project office or laboratory sponsoring (paying for) the research and development. Include address.

13. ABSTRACT: Enter an abstract giving a brief and factual summary of the document indicative of the report, even though it may also appear elsewhere in the body of the technical report. If additional space is required, a continuation sheet shall be attached.

It is highly desirable that the abstract of classified reports be unclassified. Each paragraph of the abstract shall end with an indication of the military security classification of the information in the paragraph, represented as (TS), (S), (C), or (U).

There is no limitation on the length of the abstract. However, the suggested length is from 150 to 225 words.

14. KEY WORDS: Key words are technically meaningful terms or short phrases that characterize a report and may be used as index entries for cataloging the report. Key words must be selected so that no security classification is required. Identifiers, such as equipment model designation, trade name, military project code name, geographic location, may be used as key words but will be followed by an indication of technical context. The assignment of links, roles, and weights is optional.